

Short Note

N^1 -{4-[2-(Methylthio)-1*H*-imidazol-5-yl]pyridin-2-yl}benzene-1,4-diamine

Ahmed El-Gokha ^{1,2}, Francesco Ansideri ¹, Stanislav Andreev ¹, Dieter Schollmeyer ³, Stefan Laufer ¹  and Pierre Koch ^{1,4,*} 

¹ Department of Pharmaceutical Chemistry, Institute of Pharmaceutical Sciences, Eberhard Karls Universität Tübingen, Auf der Morgenstelle 8, 72076 Tübingen, Germany; ahmed.abdelaleem@science.menofia.edu.eg (A.E.-G.); francesco.ansideri@uni-tuebingen.de (F.A.); stanislav.andreev@uni.tuebingen.de (S.A.); stefan.laufer@uni-tuebingen.de (S.L.)

² Chemistry Department, Faculty of Science, Menofia University, Gamal Abdel-Nasser Street, 32511 Shebin El-Koum, Menofia, Egypt

³ Department of Organic Chemistry, Johannes Gutenberg-University Mainz, Duesbergweg 10-14, 55099 Mainz, Germany; scholli@uni-mainz.de

⁴ Department of Pharmaceutical/Medicinal Chemistry II, Institute of Pharmacy, University of Regensburg, Universitätsstraße 31, 93053 Regensburg, Germany

* Correspondence: pierre.koch@uni-tuebingen.de; Tel.: +49-7071-29-74579

Received: 22 December 2018; Accepted: 12 February 2019; Published: 20 February 2019



Abstract: The title compound N^1 -{4-[2-(methylthio)-1*H*-imidazol-5-yl]pyridin-2-yl}benzene-1,4-diamine (**2**) was synthesized via nucleophilic aromatic substitution of 2-chloro-4-[2-(methylthio)-1*H*-imidazol-5-yl]pyridine (**3**) and *p*-phenylenediamine under acidic conditions. The synthesized compound **2** was characterized by ¹H-NMR, ¹³C-NMR, MS HPLC, IR and UV-VIS. Additionally, the structure of **2** was confirmed by single crystal X-ray diffraction. Pyridinylimidazole **2** displays moderate affinity towards the c-Jun N-terminal kinase 3 and shows selectivity versus the closely related p38 α mitogen-activated protein kinase.

Keywords: pyridinylimidazole; kinase inhibitor; c-Jun N-terminal kinase 3; JNK3; heterocycle; single crystal diffraction

1. Introduction

2-Alkylsulfanylimidazoles represent an important class of kinase inhibitors [1]. Most of the reported compounds belonging to this class have been reported as potent reversible inhibitors of p38 α mitogen-activated protein (MAP) kinase displaying IC₅₀ values down to the low nanomolar range [2–6]. In addition, several 2-alkylsulfanylimidazoles were employed in recent studies as lead structures for the design of inhibitors of other protein kinases not belonging to the MAP kinase family, e.g. the epidermal growth factor receptor kinase (EGFR) [7,8] as well as the protein kinases CK1 δ and CK1 ϵ [9].

N^1 -{4-[4-(4-Fluorophenyl)-2-(methylthio)-1*H*-imidazol-5-yl]pyridin-2-yl}benzene-1,4-diamine (**1**) was synthesized in our group and served as a lead compound for the design of both reversible and covalent c-Jun N-terminal kinase 3 (JNK3) inhibitors [10,11] as well as representing a precursor for fluorescein-labelled pyridinylimidazole PIT0105006, which is used as a reporter molecule in different fluorescence polarization-based binding assays [12,13].

Pyridinylimidazole **1** is a potent dual p38 α MAP kinase/JNK3 inhibitor displaying IC₅₀ values of 17 and 24 nM, respectively, in the corresponding activity assays. To estimate the contribution of the 4-fluorophenyl ring to the inhibitory activity, this moiety was removed resulting in the title compound **2** (Figure 1).

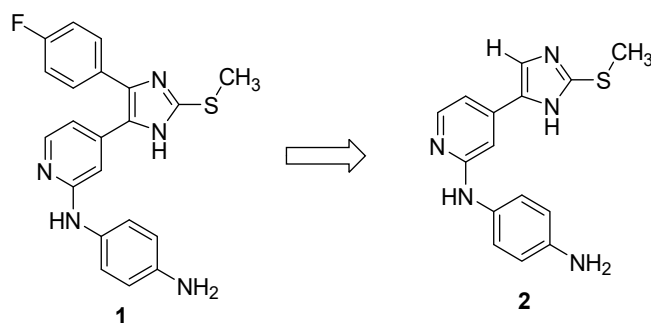
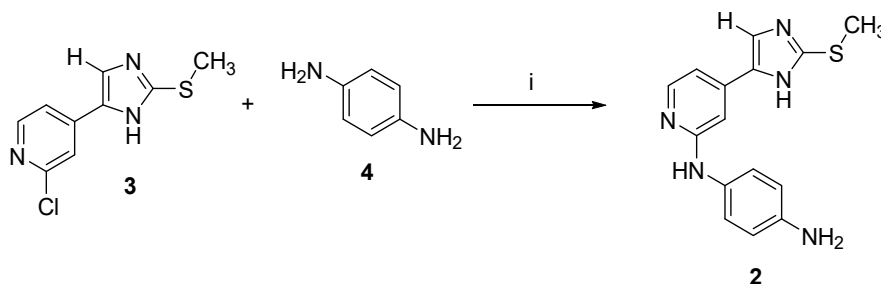


Figure 1. Structure of dual p38 α mitogen-activated protein (MAP) kinase/c-Jun N-terminal kinase 3 (JNK3) inhibitor **1** and design of the title compound **2**.

2. Results and Discussion

2.1. Chemistry

The synthesis of the new compound *N*¹-[4-[2-(methylthio)-1*H*-imidazol-5-yl]pyridin-2-yl]benzene-1,4-diamine (**2**) is depicted in Scheme 1. 2-Chloro-4-[2-(methylthio)-1*H*-imidazol-5-yl]pyridine (**3**) was reacted with *p*-phenylenediamine (**4**) in a pressure tube for 12 h at 180 °C using an ethanolic HCl solution as solvent. The reaction was concentrated under reduced pressure and the residue was purified twice by flash-column chromatography. The chemical structure of **2** was determined by ¹H-nuclear magnetic resonance spectroscopy (NMR), ¹³C-NMR MS, IR, UV-VIS and X-ray diffraction (Figure 2) and its purity was analyzed by high performance liquid chromatography (HPLC).



Scheme 1. Synthesis of *N*¹-[4-[2-(methylthio)-1*H*-imidazol-5-yl]pyridin-2-yl]benzene-1,4-diamine (**2**).
(i) 1.25 M HCl in EtOH, 12 h, 180 °C.

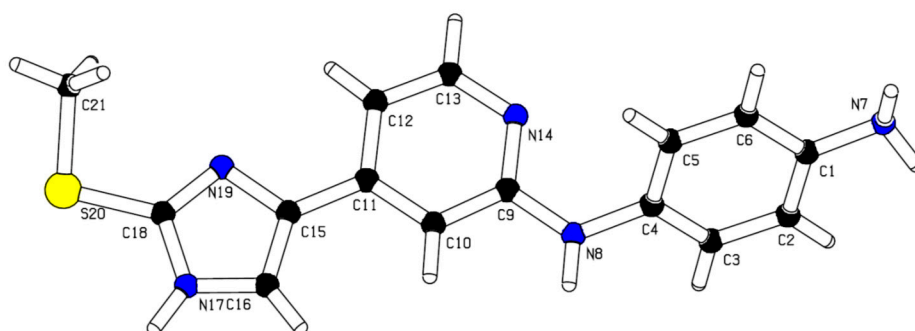


Figure 2. Crystal structure of the title compound **2**.

2.2. Biological Activity

Pyridinylimidazole **2** was evaluated in enzyme-linked immunosorbent assays [14–17] for its ability to inhibit the MAP kinases JNK3 and p38 α MAP kinase (Table 1) and its biological activities were compared to compound **1** (Table 1).

Table 1. Evaluation of pyridinylimidazoles **1** and **2** for p38 α MAP kinase and JNK3 inhibition.

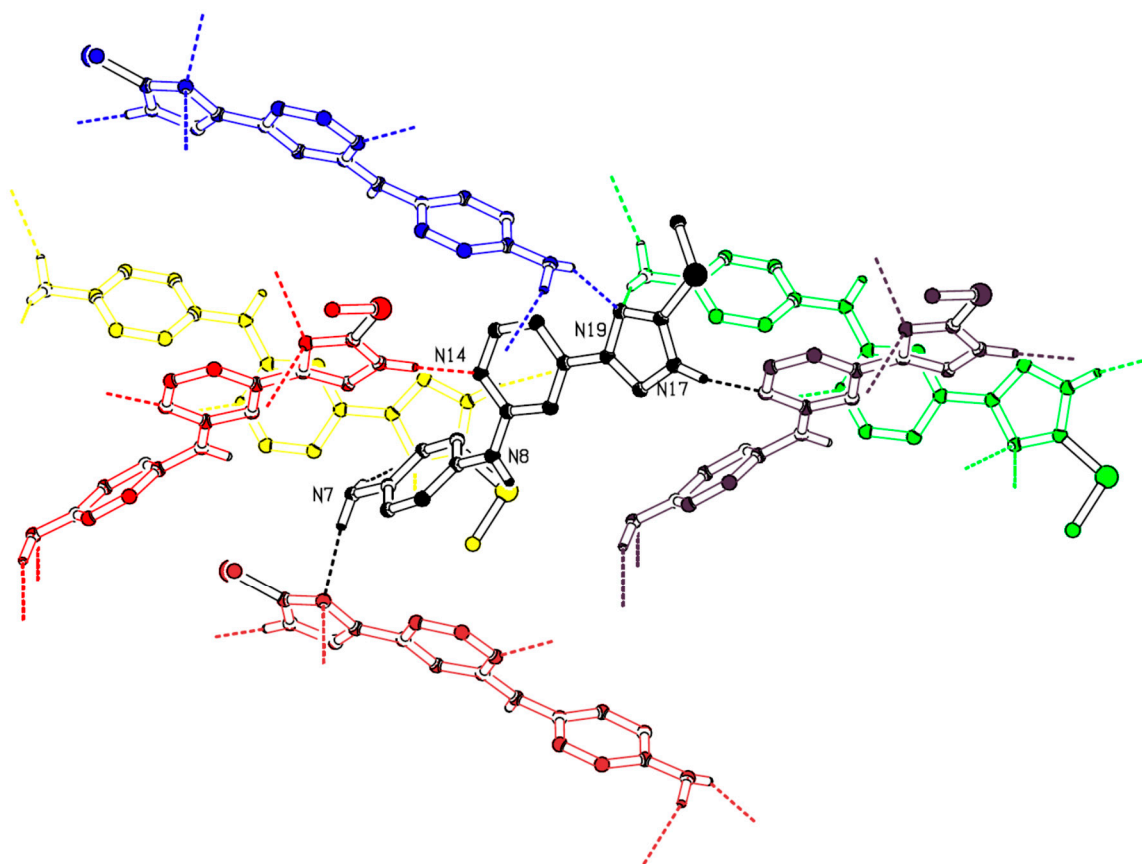
Compound	IC ₅₀ (nM) ^a	
	p38 α MAP kinase ^b	JNK3 ^c
1	17	24
2	3679	410

^a n = 3; ^b ATP concentration: 100 μ M; ^c ATP concentration: 10 μ M.

The removal of the 4-fluorophenyl moiety present in parent compound **1** resulted in a >200-fold decreased inhibitory activity on p38 α MAP kinase, whereas in the case of JNK3 only a 17-fold drop in potency was observed. Pyridinylimidazole **2** inhibited JNK3 in the triple-digit nanomolar range and displayed selectivity versus the closely related p38 α MAP kinase.

2.3. X-Ray Structure

The crystal packing of **2** features numerous hydrogen bonds, generating a three-dimensional network (Figure 3). The imidazole N–H group (N17–H) acts as a hydrogen bond donor for an interaction to the pyridine–N atom (N14) of another molecule. The imidazole N atom (N19) accepts two hydrogen bonds from the primary amine (N7–H₂) of two different molecules.

**Figure 3.** Partial packing diagram of **2**. Intermolecular hydrogen bonds are indicated as dashed lines.

The benzene ring makes dihedral angles of 56.25(15) $^\circ$ and 57.72(15) $^\circ$ with the pyridine ring and imidazole ring, respectively. The pyridine ring is almost in a parallel orientation to the imidazole ring (dihedral angles: 1.69(15) $^\circ$).

3. Materials and Methods

3.1. General

All reagents and solvents were of commercial quality and utilized without further purification. The purity of the title compound **2** was determined by reverse phase HPLC (Agilent Technologies, Santa Clara, CA, USA). An Agilent 1100 Series HPLC system was used, equipped with a UV DAD (detection at 218, 254 and 280 nm). The chromatographic separation was performed on an XBridge™ C18 column (150 × 4.6 mm, 5 μm) at 30 °C oven temperature. The injection volume was 10 μL and the flow was 1.5 mL/min using the following gradient: 0.01 M KH₂PO₄, pH 2.3 (solvent A), MeOH (solvent B), 45% B to 85% B in 9 min; 85% B for 6 min; stop time 16 min. Column chromatography was performed on Davisil LC₆₀A 20–45 μm silica from Grace Davison and Geduran Si₆₀ 63–200 μm silica from Merck (Merck, Darmstadt, Germany) for the pre-column using an Interchim PuriFlash 430 automated flash chromatography system. NMR spectra were measured on a Bruker Avance NMR spectrometer (Bruker Daltonik GmbH, Bremen, Germany) at 400 MHz. Chemical shifts are reported in parts per million (ppm) relative to tetramethylsilane. All spectra were calibrated against the (residual proton) peak of the deuterated solvent used. Mass spectra were performed on an Advion Expression S electrospray ionization mass spectrometer (ESI-MS) (Advion, Ithaca, NY, USA) with TLC interface. Melting point was determined on a Mettler Toledo MP70 Melting Point System (Mettler Toledo, LLC, Columbus, OH, USA). The IR spectra was recorded on a Thermo Scientific Nicolet 380 FT-IR (Thermo Fisher Scientific, Waltham, MA, USA) using ATR technology and strong, medium and weak peaks are represented by s, m and w, respectively. The UV-VIS spectrum was measured on a VWR UV-1600PC Spectrophotometer (VWR international GmbH, Darmstadt, Germany). X-ray diffraction data were collected on a STOE IPDS 2T diffractometer (Stoe & Cie GmbH, Darmstadt, Germany) using monochromated Mo K α radiation (0.71073 Å).

3.2. Chemistry

In a pressure vial 2-chloro-4-[2-(methylthio)-1*H*-imidazol-5-yl]pyridine (**3**)¹¹ (248 mg, 1.1 mmol) and *p*-phenylenediamine (**4**) (154 mg, 1.5 mmol) was dissolved in *n*-butanol and 1.25 M HCl in EtOH (880 μL, 1.1 mmol) was added in one portion. The vial was tightly closed, and the reaction was heated at 180 °C and stirred for 12 h. The solvent was evaporated at reduced pressure and the residue was purified twice by flash column chromatography (SiO₂, DCM/EtOH gradient elution from 97:03 to 50:50 and SiO₂, DCM/EtOH 85:15) to yield 165 mg (50%) of the title compound **2**. Brown block crystals of **2** suitable for X-ray determination were obtained by slow evaporation of a solution of the solid in ethanol at 25 °C. Mp. 204 °C; ¹H-NMR (400 MHz, DMSO-*d*₆) δ 2.57 (s, 3H), 4.73 (br. s, 2H, exchangeable), 6.52 (d, *J* = 8.6 Hz, 2H), 6.89 (d, *J* = 5.1 Hz, 1H), 7.07 (s, 1H), 7.23 (d, *J* = 8.3 Hz, 2H), 7.73 (s, 1H), 7.94 (d, *J* = 5.3 Hz, 1H), 8.40 (s, 1H, exchangeable), 12.42 (br. s, 1H, exchangeable); ¹³C-NMR (101 MHz, DMSO-*d*₆) δ 15.3 (CH₃), 103.2 (CH), 108.9 (CH), 114.2 (CH), 116.6 (Cq), 121.3 (CH), 131.0 (Cq), 139.3 (Cq), 141.8 (Cq), 141.9 (Cq), 143.1 (Cq), 147.3 (CH), 157.5 (Cq); IR (ATR) 3387m, 3305w (NH₂), 3220w (NH₂), 3146w (CHAr), 2921w (CH), 1605s, 1573m (C-C Ar), 1516s, 1487s, 1430s, 1082m, 825m, 788s, 514m, 465 cm⁻¹; UV-VIS: λ_{max} 267 nm (log ϵ = 73.98) in methanol; ESI-MS: (*m/z*) 296.2 [M – H]⁻, 298.2 [M + H]⁺; HPLC: *t*_r = 1.860 min (purity 100%, 254 nm; purity 97.8%, 280 nm). Crystal data for C₁₅H₁₅N₅S (M = 297.38 g·mol⁻¹): Orthorhombic space group Pbc_a, *a* = 17.0850 (8) Å, *b* = 9.5083 (4) Å, *c* = 18.1054 (7) Å, *V* = 2941.2 (2) Å³, *Z* = 8, *T* = 193 K, μ (MoK α) = 0.22 mm⁻¹, *D*_{calc} = 1.343 m·gm⁻³, 8551 reflections measured (2.4° ≤ θ ≤ 27.9°), 3502 unique (*R*_{int} = 0.1557, *R*_{sigma} = 0.0607) which were used in all calculations. CCDC 1895079 contains the supplementary crystallographic data for this paper. These data can be obtained free of charge via <http://www.ccdc.cam.ac.uk/conts/retrieving.html>.

4. Conclusions

The synthesis of N^1 -[4-[2-(methylthio)-1*H*-imidazol-5-yl]pyridin-2-yl]benzene-1,4-diamine (**2**) was performed via nucleophilic aromatic substitution of 2-chloro-4-[2-(methylthio)-1*H*-imidazol-5-yl]pyridine (**3**) and *p*-phenylenediamine (**4**) under acidic conditions. The analytical characterization of the novel compound **2** comprised $^1\text{H-NMR}$, $^{13}\text{C-NMR}$, MS, HPLC, IR, UV-VIS and single crystal X-ray diffraction. Biological evaluation revealed pyridinylimidazole **2** to be a moderate inhibitor of JNK3 displaying selectivity versus the closely related p38 α MAP kinase.

Supplementary Materials: The following are available online, Figure S1: $^1\text{H-NMR}$ of **2**; Figure S2: $^{13}\text{C-NMR}$ of **2**; Figure S3: ESI-MS of **2**; Figure S4: HPLC of **2**; Figure S5: IR of **2**; Figure S6: UV-VIS of **2**.

Author Contributions: A.E.-G., F.A., S.A., S.L. and P.K. conceived and designed the experiments; A.E.-G. performed the synthesis; A.E.-G., F.A., S.A., D.S. and P.K. analyzed the data; P.K. wrote the paper.

Funding: This research received no external funding.

Conflicts of Interest: The authors declare no conflict of interest.

References

1. Koch, P.; Ansideri, F. 2-Alkylsulfanyl-4(5)-aryl-5(4)-heteroaryl-imidazoles: An Overview on Synthetic Strategies and Biological Activity. *Arch. Pharm.* **2017**, *350*, e1700258. [[CrossRef](#)] [[PubMed](#)]
2. Koch, P.; Bäuerlein, C.; Jank, H.; Laufer, S. Targeting the ribose and phosphate binding site of p38 mitogen-activated protein (MAP) kinase: Synthesis and biological testing of 2-alkylsulfanyl-, 4(5)-aryl-, 5(4)-heteroaryl-substituted imidazoles. *J. Med. Chem.* **2008**, *51*, 5630–5640. [[CrossRef](#)] [[PubMed](#)]
3. Laufer, S.; Hauser, D.; Stegmüller, T.; Bracht, C.; Ruff, K.; Schattel, V.; Albrecht, W.; Koch, P. Tri- and tetrasubstituted imidazoles as p38 α mitogen-activated protein kinase inhibitors. *Bioorg. Med. Chem. Lett.* **2010**, *20*, 6671–6675. [[CrossRef](#)] [[PubMed](#)]
4. Laufer, S.; Koch, P. Towards the improvement of the synthesis of novel 4(5)-aryl-5(4)-heteroaryl-2-thio-substituted imidazoles and their p38 MAP kinase inhibitory activity. *Org. Biomol. Chem.* **2008**, *6*, 437–439. [[CrossRef](#)] [[PubMed](#)]
5. Laufer, S.A.; Hauser, D.R.J.; Domeyer, D.M.; Kinkel, K.; Liedtke, A.J. Design, synthesis, and biological evaluation of novel tri- and tetrasubstituted imidazoles as highly potent and specific ATP-mimetic inhibitors of p38 MAP kinase: Focus on optimized interactions with the enzyme's surface-exposed front region. *J. Med. Chem.* **2008**, *51*, 4122–4149. [[CrossRef](#)] [[PubMed](#)]
6. Ziegler, K.; Hauser, D.R.J.; Unger, A.; Albrecht, W.; Laufer, S.A. 2-Acylaminopyridin-4-yl-imidazoles as p38 MAP Kinase Inhibitors: Design, Synthesis, and Biological and Metabolic Evaluations. *Chemmedchem* **2009**, *4*, 1939–1948. [[CrossRef](#)] [[PubMed](#)]
7. Günther, M.; Juchum, M.; Kelter, G.; Fiebig, H.; Laufer, S. Lung Cancer: EGFR Inhibitors with Low Nanomolar Activity against a Therapy-Resistant L858R/T790M/C797S Mutant. *Angew. Chem. Int. Ed.* **2016**, *55*, 10890–10894. [[CrossRef](#)] [[PubMed](#)]
8. Günther, M.; Lategahn, J.; Juchum, M.; Döring, E.; Keul, M.; Engel, J.; Tumbrink, H.L.; Rauh, D.; Laufer, S. Trisubstituted Pyridinylimidazoles as Potent Inhibitors of the Clinically Resistant L858R/T790M/C797S EGFR Mutant: Targeting of Both Hydrophobic Regions and the Phosphate Binding Site. *J. Med. Chem.* **2017**, *60*, 5613–5637. [[CrossRef](#)] [[PubMed](#)]
9. Halekotte, J.; Witt, L.; Ianes, C.; Krüger, M.; Bührmann, M.; Rauh, D.; Pichlo, C.; Brunstein, E.; Luxenburger, A.; Baumann, U.; Knippschild, U.; Bischof, J.; Peifer, C. Optimized 4,5-Diarylimidazoles as Potent/Selective Inhibitors of Protein Kinase CK1 δ and Their Structural Relation to p38 α MAPK. *Molecules* **2017**, *22*, 522. [[CrossRef](#)] [[PubMed](#)]
10. Muth, F.; El-Gokha, A.; Ansideri, F.; Eitel, M.; Döring, E.; Sievers-Engler, A.; Lange, A.; Boeckler, F.M.; Lämmerhofer, M.; Koch, P.; Laufer, S.A. Tri- and Tetrasubstituted Pyridinylimidazoles as Covalent Inhibitors of c-Jun N-Terminal Kinase 3. *J. Med. Chem.* **2017**, *60*, 594–607. [[CrossRef](#)] [[PubMed](#)]

11. Ansideri, F.; Macedo, J.T.; Eitel, M.; El-Gokha, A.; Zinad, D.S.; Scarpellini, C.; Kudolo, M.; Schollmeyer, D.; Boeckler, F.M.; Blaum, B.S.; Laufer, S.A.; Koch, P. Structural optimization of a pyridinylimidazole scaffold: shifting the selectivity from p38 α mitogen-activated protein kinase to c-Jun N-terminal kinase 3. *ACS Omega* **2018**, *3*, 7809–7831. [[CrossRef](#)] [[PubMed](#)]
12. Ansideri, F.; Dammann, M.; Boeckler, F.M.; Koch, P. Fluorescence polarization-based competition binding assay for c-Jun N-terminal kinases 1 and 2. *Anal. Biochem.* **2017**, *532*, 26–28. [[CrossRef](#)] [[PubMed](#)]
13. Ansideri, F.; Lange, A.; El-Gokha, A.; Boeckler, F.M.; Koch, P. Fluorescence polarization-based assays for detecting compounds binding to inactive c-Jun N-terminal kinase 3 and p38 alpha mitogen-activated protein kinase. *Anal. Biochem.* **2016**, *503*, 28–40. [[CrossRef](#)] [[PubMed](#)]
14. Goettert, M.; Graeser, R.; Laufer, S.A. Optimization of a nonradioactive immunosorbent assay for p38alpha mitogen-activated protein kinase activity. *Anal. Biochem.* **2010**, *406*, 233–234. [[CrossRef](#)] [[PubMed](#)]
15. Goettert, M.; Luik, S.; Graeser, R.; Laufer, S.A. A direct ELISA assay for quantitative determination of the inhibitory potency of small molecules inhibitors for JNK3. *J. Pharma. Biomed. Anal.* **2011**, *55*, 236–240. [[CrossRef](#)] [[PubMed](#)]
16. Peifer, C.; Luik, S.; Thuma, S.; Herwey, Y.; Graeser, R.; Laufer, S.A. Development and optimization of a non-radioactive JNK3 assay. *Comb. Chem. High Throughput Screen.* **2006**, *9*, 613–618. [[CrossRef](#)] [[PubMed](#)]
17. Laufer, S.; Thuma, S.; Peifer, C.; Greim, C.; Herweh, Y.; Albrecht, A.; Dehner, F. An Immunosorbent, Nonradioactive p38 Map Kinase Assay Comparable to Standard Radioactive Liquid-Phase Assays. *Anal. Biochem.* **2005**, *344*, 135–137. [[CrossRef](#)] [[PubMed](#)]



© 2019 by the authors. Licensee MDPI, Basel, Switzerland. This article is an open access article distributed under the terms and conditions of the Creative Commons Attribution (CC BY) license (<http://creativecommons.org/licenses/by/4.0/>).